Desalination and Water Treatment
www.deswater.com

doi: 10.5004/dwt.2021.26472

209 (2021) 334–341
January

Effects of chlorella extracellular polymeric substances on the aggregation and stability of TiO_2 nanoparticles as electrolytes

Yanyan Zhang, Xuankun Li*, Juan Du, Lihui Pu, Sihao Chen*

College of Chemistry and Chemical Engineering, Shanghai University of Engineering Science, Shanghai 201620, China, emails: li.xuankun@sues.edu.cn (X. Li), chensh@sues.edu.cn (S. Chen), zhangyanyan@163.com (Y. Zhang), bairuochen12@163.com (J. Du), 708877376@qq.com (L. Pu)

Received 16 February 2020; Accepted 18 August 2020

ABSTRACT

The enormous application of commercial TiO_2 nanoparticles (TiO_2 NPs) in industrial products will potentially lead to release of TiO_2 NPs in the environment. The aggregation and stability of TiO_2 NPs in natural aquatic environments are essential in assessing their environmental risks. This paper explores the effects of *Chlorella* extracellular polymeric substances (EPS) on the aggregation and stability of TiO_2 NPs as electrolytes. It was found that an increase in NaCl concentration from 0 to 70 mM, the introduction of 5 mg/L EPS better retarded the decline of the absolute zeta potential of TiO_2 NPs than 1 mg/L EPS. In addition, the critical coagulation concentration and stability of TiO_2 NPs also increased with the concentration of EPS. The synergistic effects of steric hindrance and electrostatic repulsion exerted by EPS is considered to stabilize the TiO_2 NPs in NaCl electrolyte medium. However, when using $CaCl_2$ as the background electrolyte, the polysaccharide groups of EPS can be bridged by Ca^{2+}, promoting the aggregation and decreasing the stability of TiO_2 NPs. This study investigates the effects of EPS on the aggregation and stability of TiO_2 NPs, which can vary significantly with change in valency and concentration of the electrolyte, making it crucial to understanding the fate and accessing the risks of applying TiO_2 NPs in natural water matrices.

Keywords: Chlorella EPS; TiO_2 nanoparticle; Electrolyte; Aggregation; Stability

1. Introduction

Due to their unique physicochemical properties, engineered nanoparticles (ENPs) are frequently employed in industrial practices and daily life. It was estimated by Nowack and Bucheli [1] that the productivity of ENPs will go up to 58,000 tons by 2020 based on the employment of nanomaterials in previous years. ENPs are likely to enter the environment via industrial and domestic wastewater, sludge of wastewater treatment plant and waste incineration residues [2].

Among all ENPs, titanium dioxide nanoparticle is one of the most widely used nanomaterials. TiO_2 NPs has many uses, including to fabricate photocatalysts, solar cells, paints, personal care products, and so on. Wastewater from domestic sewage treatment plants usually contains nano-TiO_2. Keller et al. [3] estimated that the nano-TiO_2 released into sewage system can reach 870–1,000 tons a year in the United States. In recent years, more, and more researchers are focusing on the ecotoxicity of ENPs. For example, Jia et al. [4] evaluated the effects of TiO_2 nanoparticles and multi-walled carbon nanotubes on the freshwater diatoms. It was found that different exposure time and concentration of the nanomaterials will lead to different physiological and biochemical effects on freshwater diatoms. Liu et al. [5] studied the effects of crystalline forms of TiO_2 NPs on the physiological parameters of *Daphnia magna*, and found that anatase TiO_2 NPs may cause more severe damages

* Corresponding authors.

to aquatic organisms at the same bioaccumulation level. Hu et al. [6] reported that TiO_2 NPs can act as an effective carrier for lead to increase its uptake, bioavailability, and toxicity in zebrafish embryos.

ENPs possess more reactive sites than other contaminants due to their small particle sizes and large specific surface area [7–9]. Once released into the environment, ENPs will interact with environmental components such as natural organic matter or inorganic ions [10–12]. Many studies have proved that the bioavailability and toxicity of ENPs to the organism are highly correlated with their particle sizes and colloidal stability. The environmental behavior of ENPs such as aggregation and sedimentation could remarkably affect the fate and ecotoxicity [13–15]. Some researchers have clarified that the electrostatic force and steric hindrance between nanoparticles will change in the presence of natural organic matter and electrolytes, significantly affecting colloidal stability of nanoparticles [16–21] as a result.

Extracellular polymeric substances (EPS) are common components of the natural environmental organic matter. EPS are the mixture of biomacromolecules, produced by microbes during growth and metabolism [22]. As the matrix of biofilms [23], EPS mainly consists of polysaccharides, proteins, small amounts of nucleic acids, and esters [24,25]. In natural water, much of the total extracellular organic substances were secreted by algae, a crucial part of natural organic matter that plays an important role in the aquatic environment. Adeleye et al. [26] studied the effects of EPS on long-term colloidal stability and metal leaching of single-walled carbon nanotubes, which have demonstrated the improved stability of CNTs by EPS in comparison to Suwanee River natural organic matter. Xu and Jiang [27] investigated the stability of ZnO nanoparticles after adsorption of cyanobacterial EPS, and found that the turbidity of ZnO nanoparticles solutions increased with the introduction of EPS, which has demonstrated that the colloidal stability of ZnO nanoparticles had been enhanced. Kroll et al. [28] found that CeO_2 NPs were stabilized by EPS, and the process would not be affected by pH or illumination. Although many studies have shown the effects of EPS on the aggregation and stability of ENPs, the real natural water matrices are more complicated, and the co-effects of electrolytes and EPS on the environmental behavior of NPs lack sufficient research.

Degussa P25 nano-TiO_2 is commercially available and proven to show good photoactivity, so it has been widely used in laboratory and industries [29]. In this study, typical P25 TiO_2 NPs were selected as the targeted nanoparticle, and the effects of *Chlorella* EPS as different electrolytes were investigated. Firstly, zeta potential was determined to study the effects of EPS on the surface charge of TiO_2 NPs. Secondly, the dynamic light scattering (DLS) was applied to study the aggregation kinetics of TiO_2 NPs in the presence and absence of EPS as the valence and concentration of electrolyte. Finally, the effects of EPS on the stability of TiO_2 NPs as electrolytes were studied through monitoring the absorbance of TiO_2 by using an ultraviolet spectrophotometer for 12 h with different intervals. This study provides an important reference for estimating the fate and transport of ENPs in the natural aquatic environment.

2. Materials and methods

2.1. Preparation of TiO_2 NPs stock solution

Titanium dioxide (TiO_2) NPs were purchased from Sigma-Aldrich (USA) with >99.5% purity, the primary average particle size was 21 nm. To prepare the nanoparticle suspension, 20 mg of the nanoparticle powder was added to 100 mL of ultrapure water and was sonicated for 30 min. The stock solution was stored at 4°C and was sonicated for 30 min before being used.

2.2. Initial characterization of TiO_2 NPs

Powder X-ray diffraction (XRD) of the TiO_2 NPs was performed on a Bruker D2 advance diffractometer (Bruker AXS Gmbh, Karlsruhe, Germany). The shape and morphology of TiO_2 NPs were observed through a scanning electron microscopy (SEM, Hitachi S4800, Japan) with selected area electron diffraction. The size of TiO_2 NPs was confirmed by transmission electronic microscopy (TEM, JEM-2100, JEOL, Japan) (Fig. 1). Initially, TiO_2 NPs dispersed in ultrapure water were imaged through transmission electron microscopy (TEM) by depositing of 10 μL drop on formvar/carbon-coated copper grids and then drying overnight. After that, micrographs were obtained at 200 keV. The hydrodynamic diameter of the TiO_2 nanoparticle was determined by using dynamic light scattering (Zetasizer Nano-S90, Malvern Instruments Ltd., UK) at 25°C.

2.3. EPS extraction

Chlorella vulgaris (FACHB-1068 in this study was obtained from the freshwater algae culture collection at the Institute of Hydrobiology (FACHB, Wuhan, China), and EPS was extracted from *Chlorella* by centrifugation [27]. In brief, the purchased algae liquid was transferred to a conical flask containing BG-11 medium. The organisms were cultured under cool white LED lights with a photoperiod of 12:12 h light-dark cycle, at 25°C ± 0.5°C until reaching stationary phase. Cell densities were measured using a hemocytometer. Soluble EPS fraction was harvested at the stationary growth phase and separated via centrifugation of culture solution for 30 min at 4,000 g at 4°C. The supernatant was collected and filtered by 0.22 μm needle filters (Membrane Solutions Company, US) under sterile conditions. To remove the residual of electrolyte from the growth medium and the low molecular-weight metabolites, EPS was dialyzed for 96 h at 4°C using regenerated cellulose tubular membrane of 3,500 Da cut-off (Viskase, US), and the cellulose tubular membrane was pretreated with $NaHCO_3$ and Na_2EDTA to remove impurity. The ultrapure water for dialysis was renewed every 24 h, and the EPS after dialysis was stored at 4°C until use. The total organic carbon (TOC) concentration of the EPS solution was measured by a TOC analyzer (TOC-VCPN, Shimadzu, Japan) before the experiment.

2.4. Attenuated total reflection-Fourier transform infrared spectroscopy

The dialyzed *Chlorella* EPS solution was freeze-dried to obtain dried EPS powder. The dried EPS powder was

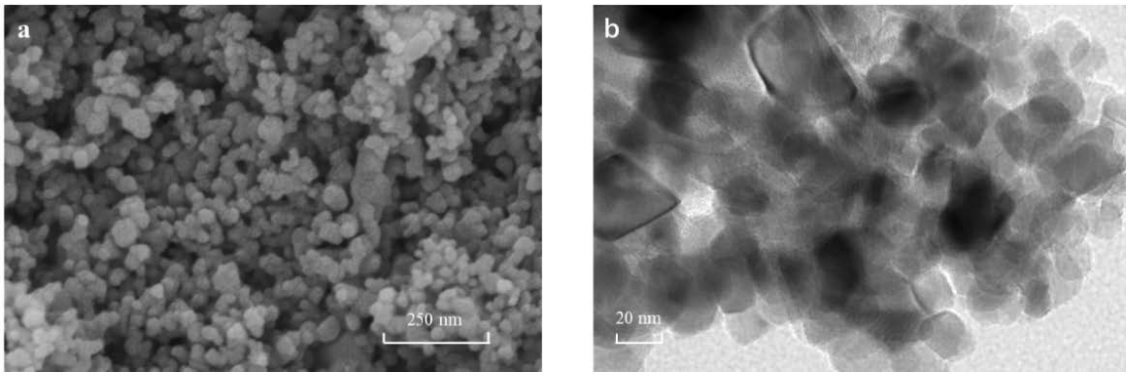

Fig. 1. SEM (a) and TEM (b) images of TiO_2 NPs.

deposited on a KBr crystal in a Fourier transform infrared (FTIR) spectrometer (L160-8000, PerkinElmer, MA). Each spectrum was scanned 200 times from 4,000 to 400 cm^{-1} at a resolution of 4 cm^{-1} [30].

2.5. Aggregation experiment

The change of TiO_2 hydrodynamic diameter (D_h) over time (t) was determined by dynamic light scattering (DLS) (Zetasizer Nano-S90, Malvern Instruments Ltd., UK) operating with a He–Ne laser at the wavelength of 633 nm. The TiO_2 NPs stock solution was sonicated for 30 min before the DLS measurement. The test concentrations of NaCl ranging from 1 to 60 mg/L was set at EPS concentrations of 1, 3, and 5 mg/L. The test concentrations of $CaCl_2$ ranging from 0.1 to 10 mg/L was set at EPS concentrations of 1, 3, and 5 mg/L. For each experiment, 1.2 mL of the pre-prepared mixture suspension was introduced into a cuvette (Titan, Shanghai). The concentration of TiO_2 NPs in the DLS vial was maintained at 40 mg/L. The cuvette was vortexed for 1 s right before measurement. The D_h measurement was monitored over a time period from 1 min to 60 min. During the DLS measurements, the scattered light intensity was detected by a photodetector at a scattering angle of 173°, with each autocorrelation function being accumulated over a period of 10 s. All DLS measurements were conducted under 25°C [31].

2.6. Determination of aggregation kinetics

In this study, the aggregation kinetics of TiO_2 particles in early stage could be explained as the primary rate of the increase in D_h with time t as tested by DLS. The primary aggregation rate constant (k) is proportional to the primary rate of increase in D_h and inversely proportional to the primary concentration of TiO_2 NPs in the suspension, N_0 [32,33]:

$$k \propto \frac{1}{N_0}\left(\frac{dD_h(t)}{dt}\right)_{t\to 0} \tag{1}$$

According to the method proposed by Huangfu et al. [34], the primary increase of the TiO_2 NPs D_h along with time ($dD_h(t)/dt$) was calculated during a period from aggregation initiation (t_0) to the time when D_h exceeded $1.5D_{h0}$. The value of $dD_h(t)/dt$ was obtained through linear least squares regression analysis.

The particle attachment efficiency α, which was used to quantify the aggregation kinetics of TiO_2 NPs, is determined by normalizing k gained under different solution conditions by the k_{fast} obtained under favorable (fast) aggregation conditions [33,34]:

$$\alpha = \frac{k}{k_{fast}} = \frac{\frac{1}{N_0}\left(\frac{dD_h(t)}{dt}\right)_{t\to 0}}{\left(\frac{dD_h(t)}{dt}\right)_{t\to 0,fast}} \tag{2}$$

When the primary TiO_2 concentrations N_0 were maintained constant for the measurements at different ionic strengths, Eq. (2) can be simplified by neglecting N_0 and α could be calculated by normalizing the initial slope of the aggregation profile at a given electrolyte concentration by the initial slope under favorable (fast) aggregation conditions. In order to calculate α in the presence of EPS, $(dD_h(t)/dt)_{t\to 0,fast}$ was obtained from the average values of $(dD_h(t)/dt)_{fast}$ in the diffusion-limited regime (ionic strength above the critical coagulation concentration (CCC)) in the presence of NaCl or $CaCl_2$.

2.7. Sedimentation experiments

The sedimentation of TiO_2 NPs under various electrolytes and different EPS concentration was studied by UV-vis spectroscopy (752N, Xin Mao, Shanghai). The concentration EPS was set as 0, 1, 3, and 5 mg/L in 5 mM NaCl solution and 0.5 mM $CaCl_2$ solutions, respectively. TiO_2 stock solution was sonicated for 30 min and then added into the above solution to obtain a mixture which contains 40 mg/L TiO_2 NPs. The UV-vis absorption of the suspension was measured at the wavelength of 378 nm at different time intervals within 12 h. The sedimentation of TiO_2 was expressed by A/A_0. Where A_0 is the initial absorbency and A is the absorbency recorded at different intervals during the 12 h experimental period.

2.8. Zeta potential measurement

The zeta potentials of TiO_2 and *Chlorella* EPS were determined by a Zeta potential analyzer (Zetasizer Nano ZS,

Malvern, UK). The concentrations of the *Chlorella* EPS were 1 and 5 mg/L, respectively. For ascertaining the effects of ionic strength, the concentration of NaCl or $CaCl_2$ was set in the range of 0–70 mM and pH was adjusted to 7. All the experiments were repeated three times.

3. Results and discussion

3.1. Characterization of TiO_2

The morphology of TiO_2 NPs can be observed in Figs. 1a and b. SEM of TiO_2 NPs showed a near spherical shape without obvious clumps. TEM indicated that the average size of TiO_2 NPs is close to 20 nm, which was in accordance with the size of 21 nm provided by the manufacturer. The hydrodynamic particle size was detected to be 233.6 ± 6.5 nm by DLS, and the TiO_2 surface charge was negative (–3.38 ± 0.11 mV) in neutral aqueous solution. The reason why hydrodynamic particle size of TiO_2 was much larger than the counterpart powder size might be due to the formation of TiO_2 aggregate. The zeta potential of TiO_2 was –7.38 ± 0.5 in neutral solution.

The XRD pattern of TiO_2 NPs is shown in Fig. 2a. The determined characteristic 2θ values and [hkl] planes were 25.26 [101], 37.85 [004], 47.91 [200], 53.84 [105], and 62.36 [204], which reflect the features of anatase TiO_2. The result were consistent with the standard JCPDs file number and previously published work [35,36].

3.2. Characteristics of EPS

Attenuated total reflection-Fourier transform infrared (ATR-FTIR) was applied to analyze the structure of *Chlorella* EPS, and the wave numbers from 4,400 to 400 cm^{-1} were recorded. As shown in Fig. 3, notably, the bands at 1,651; 1,574; and 1,385 cm^{-1} were assigned to the C=O of amide I, N–H of Amide II in protein, and C=O symmetric stretching vibration of –COO– groups. The bands at 1,000–1,132 cm^{-1} were ascribed to the C–O, C–C stretching vibration, C–O–C and C–O–H deformation vibrations of the polysaccharides structures. The band at 3,400 cm^{-1} was mainly attributed to –OH in carbohydrates and proteins. The FTIR spectra revealed that the *Chlorella* EPS contains a large number of functional groups that could be absorbed into the surface of the nanoparticle, hence affecting the aggregation behavior of nanoparticles in an aqueous environment.

3.3. Effects of EPS on surface charge of TiO_2 NPs as electrolyte

Surface charge is one of the determining factors in the aggregation and sedimentation behaviors of nanoparticles in aqueous solutions. Electrolytes were generally considered to compress the electric double layer of nanoparticle and lead to significant aggregation. In order to better reveal the effects of *Chlorella* EPS on the surface charge of TiO_2 NPs in a natural water environment, effects of EPS on the surface charge of TiO_2 NPs as the function of the concentration of electrolyte was studied. As shown in Fig. 4a, when the EPS concentration was 1 mg/L, with the increase of the NaCl concentrations ranging from 0 to 10 mM, the zeta potential of TiO_2 NPs changed from –22.3 to –5.3 mV. As the concentration of NaCl further increased from 10 to 70 mM, no significant variation of zeta potential could be detected. When the concentration of EPS was 5 mg/L, with the increase of the NaCl concentrations from 0 to 60 mM, the zeta potential of TiO_2 NPs shifted from –22.8 to –11.8 mV. Fig. 4b shows the effect of EPS on the zeta potential of TiO_2 NPs as the function of divalent Ca^{2+}. In the presence of 1 mg/L EPS, the zeta potential of TiO_2 NPs rise from –22.3 to +4.1 mV with the increase of $CaCl_2$ concentration from 0 to 50 mM, and the zeta potential of TiO_2 NPs in the 5 mg/L concentration of EPS mixture was –22.8 to +0.8 mV. Similarly, the absolute zeta potential of TiO_2 NPs in the 5 mg/L EPS solution with the same electrolyte concentration was significantly higher than that of TiO_2 NPs in the 1 mg/L EPS solution. When the concentration of $CaCl_2$ was

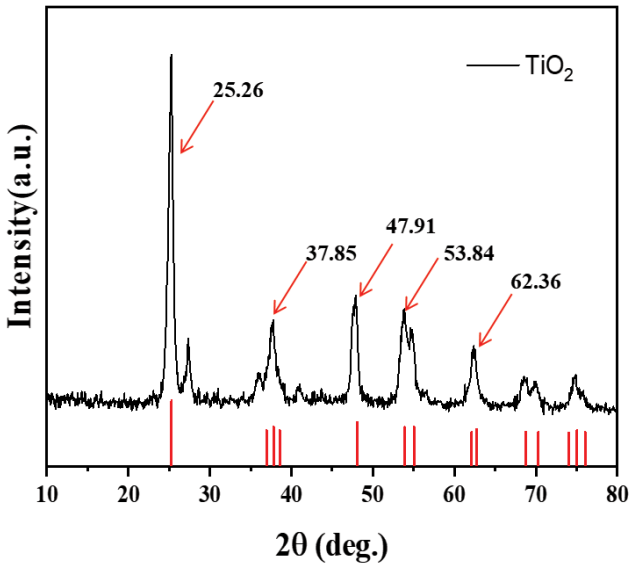

Fig. 2. X-ray diffraction pattern of TiO_2 NPs.

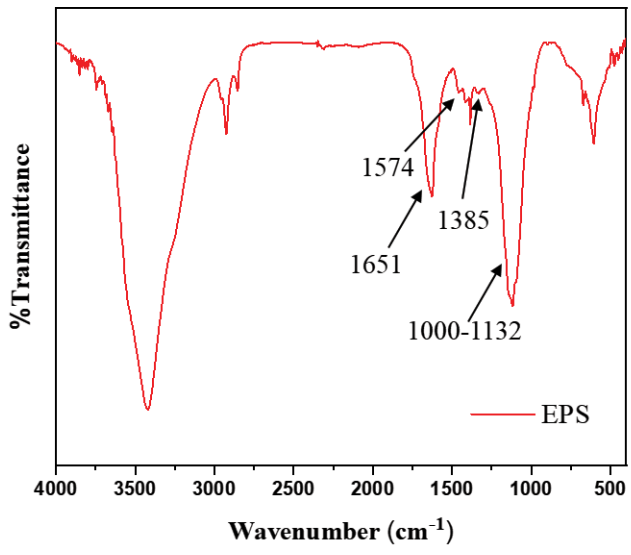

Fig. 3. FTIR spectra of EPS.

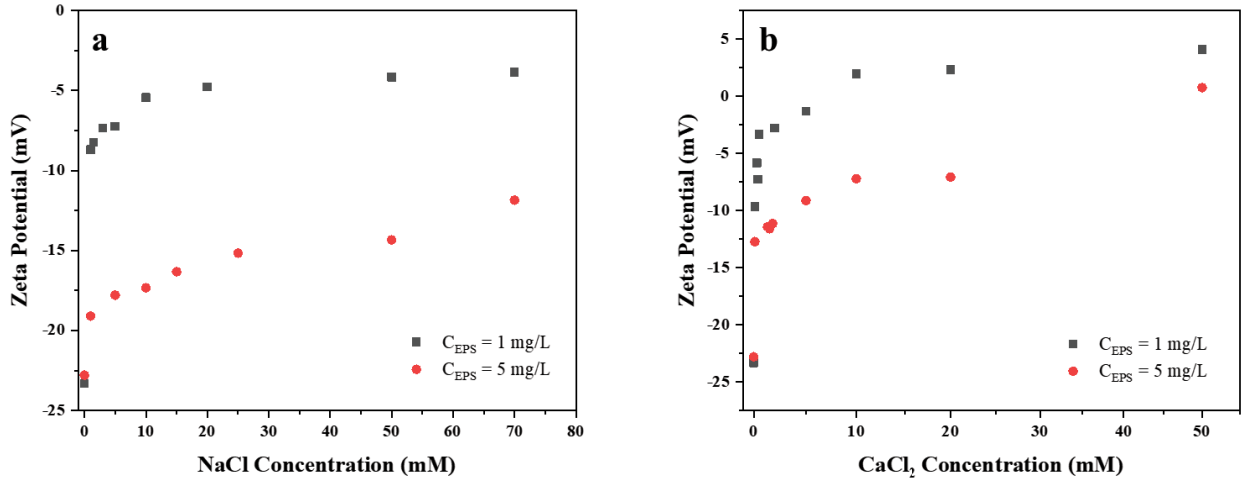

Fig. 4. Zeta potential of TiO_2 NPs in the presence of EPS as the function of (a) NaCl and (b) $CaCl_2$ concentration.

20 mM, it was obvious that the absolute zeta potential of TiO_2 NPs in 5 mg/L EPS solution was higher than that in 1 mg/L EPS solution. This phenomenon may be associated with the fact that Ca^{2+} neutralizes the negatively charged group of EPS and the surface charge of TiO_2 NPs. Therefore, the addition of *Chlorella* EPS in $CaCl_2$ solution promotes more aggregation of TiO_2 NPs than that in NaCl solution.

3.4. Effects of EPS on aggregation of TiO_2 NPs as electrolyte

The electrolyte concentration at the intersection of the reaction/diffusion-limited regimes are defined as CCC [32]. The stability of TiO_2 NPs in aquatic systems can be predicted by CCC. To explore the effects of EPS on TiO_2 NPs aggregation rate, the effects of different concentrations of EPS on the aggregation rate of TiO_2 NPs were investigated. With a background of low electrolyte concentrations, the increase in electrolyte concentration will promote the degree of charge screening and lead to an improvement in aggregation kinetics, as reflected by the rise in attachment efficiency, which was known as the reaction-limited regime ($\alpha < 1$). Under higher electrolyte concentrations, the surface charge of TiO_2 nanoparticles was almost neutralized and the energy barrier between TiO_2 nanoparticles was cleared. Therefore, the diffusion-limited aggregation ($\alpha = 1$) of nanoparticles is likely to take place. In this situation, aggregation kinetics will reach the maximum and will not be affected by the electrolyte concentration anymore.

The effects of EPS on the attachment efficiencies (α) of TiO_2 nanoparticles as electrolyte (NaCl and $CaCl_2$) solutions were shown in Fig. 5. As illustrated in Fig. 5a, in the absence of EPS, the CCC of TiO_2 NPs was 11.07 mM in NaCl solution. After the introduction of EPS with concentrations of 1, 3, and 5 mg/L, the CCC of TiO_2 NPs were determined to be 2.79, 14.99, and 23.16 mM, respectively. One milligram per liter EPS promoted the aggregation of TiO_2 NPs in NaCl solution. The point of zero charge (PZC) of TiO_2 NPs was reported to be approximately 6.2 [37], and the surface charge was 7.38 when such kind of TiO_2 NPs appeared in neutral solution. As demonstrated in Fig. 5a, when the concentration of EPS was 1 mg/L, the surface charge of TiO_2 NPs rapidly decreased with the increase in the concentration of NaCl, which was even lower than that of TiO_2 NPs in the absence of EPS, diminishing the stability of the system as a result. Despite the steric hindrance effects of EPS, the low concentration of EPS could not compensate for the electric repulsion loss caused by the neutralization of surface charge of TiO_2 NPs. The retarding effects are primarily attributed to the electrostatic repulsion. The EPS molecules absorbed on the surface of TiO_2 NPs would slow down the decline of the surface charge of TiO_2 NPs, and this phenomenon could be explained by the enhancement of the electrostatic repulsion among these NPs. Apart from this, EPS attached to the surface also provided spatial hindrance to alleviate the nanoparticles from aggregation.

As shown in Fig. 5b, the CCC of TiO_2 NPs in $CaCl_2$ solution was 3.07 mM in the absence of EPS. After the introduction of EPS with concentrations of 1, 3, and 5 mg/L, the CCC of TiO_2 NPs changed to 0.66, 1.60, and 1.69 mM, respectively. The above result indicated that the introduction of EPS promoted the aggregation of TiO_2 NPs in $CaCl_2$ containing matrices. This phenomenon may be attributed to the fact that the polysaccharide components of *Chlorella* EPS contain carboxylic groups, which could crosslink with Ca^{2+} through intermolecular reaction. Based on this, it can be inferred that in the presence of *Chlorella* EPS, the increase of the aggregation rate of TiO_2 NPs was caused by the intermolecular bridging between Ca^{2+} and the COO^- groups in the polysaccharide. Ca^{2+} complexes polysaccharide macromolecules can promote the aggregation of TiO_2 NPs, thereby speed up the growth of total agglomerates. It also has been reported that Ca^{2+} can cause aggregation of polysaccharides by intermolecular bridging of polysaccharides, which further helps to increase the polymerization of it [32–34,38,39].

3.5. Effect of EPS on stability of TiO_2 NPs as the function of electrolytes

In this section, the effects of EPS on the sedimentation behaviors of TiO_2 NPs in the electrolyte containing

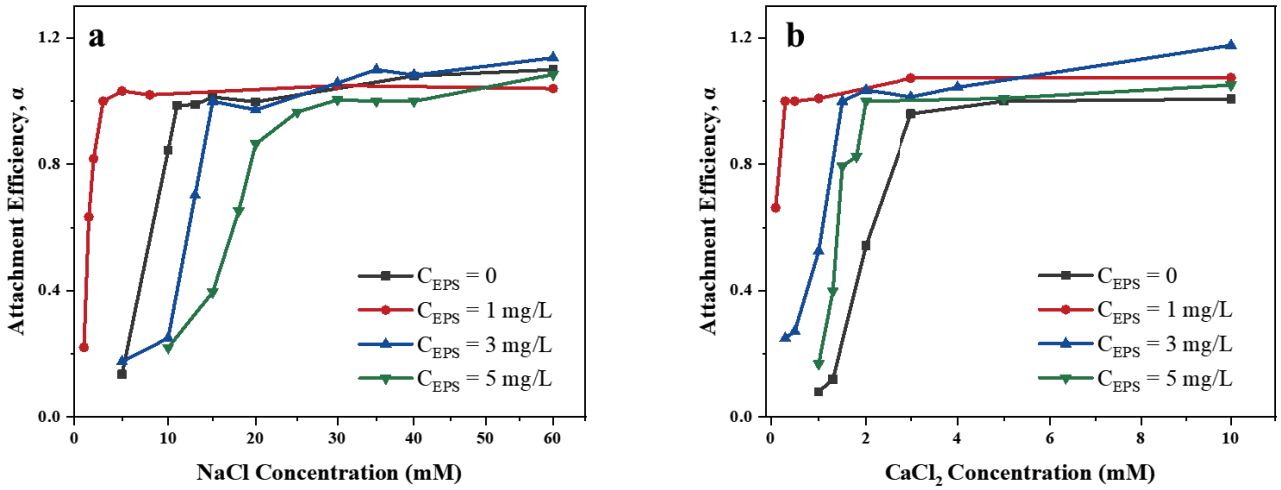

Fig. 5. CCC of TiO_2 colloids in (a) NaCl solutions and (b) $CaCl_2$ solutions.

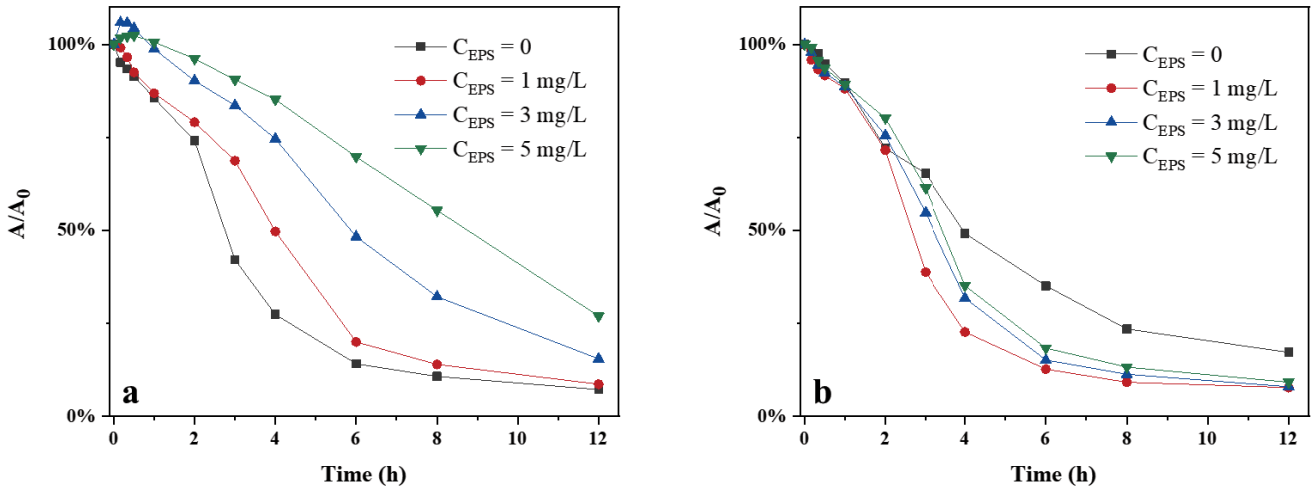

Fig. 6. Sedimentation of TiO_2 NPs in (a) 5 mM NaCl and 0.5 mM (b) $CaCl_2$.

matrices were explored. As shown in Fig. 6a, EPS remarkably retarded the sedimentation of TiO_2 NPs in an aqueous matrix containing 5 mM NaCl, and the increase rate of the retarding effect was highly correlated with the concentration of EPS. In the presence of 5 mg/L EPS, 27.0% of the TiO_2 NPs were found suspended after 12 h, 19.8% higher than the counterpart without the introduction of EPS. In NaCl solution, the EPS adsorbed on the surface of TiO_2 NPs resulted in steric hindrance, and the steric hindrance effect would enhance with the increase of EPS concentration, which impeded the sedimentation of TiO_2 NPs.

Nevertheless, as portrayed in Fig. 6b, the coexistence of EPS and divalent Ca^{2+} promoted the sedimentation of TiO_2 NPs. This result was consistent with the aggregation study, the presence of divalent Ca^{2+} bridged the EPS-covered TiO_2 nanoparticles, thereby increasing the formation of large aggregate and promoted the sedimentation process.

4. Conclusion

The effects of *Chlorella* on the aggregation behavior of TiO_2 nanoparticles were studied in the presence of different electrolytes. With regard to NaCl, the aggregation and sedimentation of TiO_2 NPs were retarded when *Chlorella* EPS concentrations were 3 or 5 mg/L. The retarding effect of nanoparticle aggregation can be attributed to the electrostatic repulsion and steric hindrance caused by EPS attached to its' surface. In comparison, when divalent Ca^{2+} was selected as the background electrolyte, the introduction of 1–5 mg/L *Chlorella* EPS promoted the aggregation and sedimentation behavior of TiO_2 NPs. This is because the EPS attached to the surface of nanoparticles contain rich polysaccharides, which can be crosslinked by Ca^{2+}. The results indicated that *chlorella* EPS has a great influence on the aggregation and sedimentation process of nanoparticles as electrolytes. This study provides an

important reference for assessing the fate and transport of ENPs in real natural waters. However, the water chemistry of natural aqueous environment is more complicated. To understand the fate of more nanoparticles in actual aquatic environment, further researches on the behaviors of ENPs in natural waters are still needed.

Acknowledgments

This work was supported by "The Innovation Action Plan of Science and Technology Commission of Shanghai Municipality of China (No. 19441901700, 19441901701, and 19441901702)".

References

[1] B. Nowack, T.D. Bucheli, Occurrence, behavior and effects of nanoparticles in the environment, Environ. Pollut., 150 (2007) 5–22.
[2] T.Y. Sun, F. Gottschalk, K. Hungerbühler, B. Nowack, Comprehensive probabilistic modelling of environmental emissions of engineered nanomaterials, Environ. Pollut., 185 (2014) 69–76.
[3] A.A. Keller, A. Lazareva, Predicted releases of engineered nanomaterials: from global to regional to local, Environ. Sci. Technol., 1 (2013) 65–70.
[4] K. Jia, C. Sun, Y. Wang, X. Li, W. Mu, Y. Fan, Effect of TiO_2 nanoparticles and multiwall carbon nanotubes on the freshwater diatom *Nitzschia frustulum*: evaluation of growth, cellular components and morphology, Chem. Ecol., 35 (2018) 69–85.
[5] S. Liu, P. Zeng, X. Li, D.Q. Thuyet, W. Fan, Effect of chronic toxicity of the crystalline forms of TiO_2 nanoparticles on the physiological parameters of *Daphnia magna* with a focus on index correlation analysis, Ecotoxicol. Environ. Saf., 181 (2019) 292–300.
[6] S. Hu, J. Han, L. Yang, S. Li, Y. Guo, B. Zhou, H. Wu, Impact of co-exposure to titanium dioxide nanoparticles and Pb on zebrafish embryos, Chemosphere, 233 (2019) 579–589.
[7] Z.G. Peng, K. Hidajat, M.S. Uddin, Adsorption of bovine serum albumin on nanosized magnetic particles, J. Colloid Interface Sci., 271 (2004) 277–283.
[8] J. Hu, G. Chen, I.M. Lo, Removal and recovery of Cr(VI) from wastewater by maghemite nanoparticles, Water Res., 39 (2005) 4528–4536.
[9] J. Lee, H.W. Walker, Adsorption of microcystin-Lr onto iron oxide nanoparticles, Colloids Surf., A, 373 (2011) 94–100.
[10] Y. Zhang, Y. Chen, P. Westerhoff, J. Crittenden, Impact of natural organic matter and divalent cations on the stability of aqueous nanoparticles, Water Res., 43 (2009) 4249–4257.
[11] F. Loosli, P. Le Coustumer, S. Stoll, TiO_2 nanoparticles aggregation and disaggregation in presence of alginate and Suwannee River humic acids pH and concentration effects on nanoparticle stability, Water Res., 47 (2013) 6052–6063.
[12] D. Palomino, S. Stoll, Fulvic acids concentration and pH influence on the stability of hematite nanoparticles in aquatic systems, J. Nanopart. Res., 15 (2013) 1428.
[13] D.A. Pelletier, A.K. Suresh, G.A. Holton, C.K. McKeown, W. Wang, B. Gu, N.P. Mortensen, D.P. Allison, D.C. Joy, M.R. Allison, S.D. Brown, T.J. Phelps, M.J. Doktycz, Effects of engineered cerium oxide nanoparticles on bacterial growth and viability, Appl. Environ. Microbiol., 76 (2010) 7981–7989.
[14] P.S. Li M, Jin X, Mädler L, Damoiseaux R, Hoek EM, Stability, bioavailability, and bacterial toxicity of ZnO and iron-doped ZnO nanoparticles in aquatic media, Environ. Sci. Technol., 45 (2011) 755–761.
[15] A.A. Keller, S. McFerran, A. Lazareva, S. Suh, Global life cycle releases of engineered nanomaterials, J. Nanopart. Res., 15 (2013) 1692.
[16] A.A. Keller, H. Wang, D. Zhou, H.S. Lenihan, G. Cherr, B.J. Cardinale, R. Miller, Z. Ji, Stability and aggregation of metal oxide nanoparticles in natural aqueous matrices, Environ. Sci. Technol., 44 (2010) 1962–1967.
[17] H.N. Kim, S.L. Walker, *Escherichia coil* O157:H7 transport in saturated porous media: role of solution chemistry and surface macromolecules, Environ. Sci. Technol., 43 (2009) 4340–4347.
[18] B.J. Thio, D. Zhou, A.A. Keller, Influence of natural organic matter on the aggregation and deposition of titanium dioxide nanoparticles, J. Hazard. Mater., 189 (2011) 556–563.
[19] M.B. Romanello, M.M. Fidalgo de Cortalezzi, An experimental study on the aggregation of TiO_2 nanoparticles under environmentally relevant conditions, Water Res., 47 (2013) 3887–3898.
[20] Y. Li, C. Yang, X. Guo, Z. Dang, X. Li, Q. Zhang, Effects of humic acids on the aggregation and sorption of nano-TiO_2, Chemosphere, 119 (2015) 171–176.
[21] A. Sheng, F. Liu, N. Xie, J. Liu, Impact of proteins on aggregation kinetics and adsorption ability of hematite nanoparticles in aqueous dispersions, Environ. Sci. Technol., 50 (2016) 2228–2235.
[22] A. Omoike, J. Chorover, Spectroscopic study of extracellular polymeric substances from *Bacillus subtilis*: aqueous chemistry and adsorption effects, Biomacromolecules, 5 (2004) 1219–1230.
[23] F. Loosli, P. Le Coustumer, S. Stoll, Effect of electrolyte valency, alginate concentration and pH on engineered TiO_2 nanoparticle stability in aqueous solution, Sci. Total Environ., 535 (2015) 28–34.
[24] B. Cao, L. Shi, R.N. Brown, Y. Xiong, J.K. Fredrickson, M.F. Romine, M.J. Marshall, M.S. Lipton, H. Beyenal, Extracellular polymeric substances from *Shewanella* sp. HRCR-1 biofilms: characterization by infrared spectroscopy and proteomics, Environ. Microbiol., 13 (2011) 1018–1031.
[25] A. Omoike, J. Chorover, Adsorption to goethite of extracellular polymeric substances from Bacillus subtilis, Geochim. Cosmochim., 70 (2006) 827–838.
[26] A.S. Adeleye, A.A. Keller, Long-term colloidal stability and metal leaching of single wall carbon nanotubes: effect of temperature and extracellular polymeric substances, Water Res., 49 (2014) 236–250.
[27] H. Xu, H. Jiang, Effects of cyanobacterial extracellular polymeric substances on the stability of ZnO nanoparticles in eutrophic shallow lakes, Environ. Pollut., 197 (2015) 231–239.
[28] A. Kroll, R. Behra, R. Kaegi, L. Sigg, Extracellular polymeric substances (EPS) of freshwater biofilms stabilize and modify CeO_2 and Ag nanoparticles, PLoS One, 9 (2014) e110709.
[29] D.C. Huram, A.G. Agrios, K.A. Gray, T. Rajh, M.C. Thurnauer, Explaining the enhanced photocatalytic activity of degussa P25 mixed-phase TiO_2 using EPR, J. Phys. Chem. B, 107 (2003) 4545–4549.
[30] L.Y. Ren, Z.N. Hong, W. Qian, J.Y. Li, R.K. Xu, Adsorption mechanism of extracellular polymeric substances from two bacteria on ultisol and alfisol, Environ. Pollut., 237 (2018) 39–49.
[31] D. Lin, S. Drew Story, S.L. Walker, Q. Huang, P. Cai, Influence of extracellular polymeric substances on the aggregation kinetics of TiO_2 nanoparticles, Water Res., 104 (2016) 381–388.
[32] K.L. Chen, M. Elimelech, Aggregation and deposition kinetics of fullerene (C_{60}) nanoparticles, Langmuir, 26 (2006) 10994–11001.
[33] K.L. Chen, M. Elimelech, Influence of humic acid on the aggregation kinetics of fullerene (C_{60}) nanoparticles in monovalent and divalent electrolyte solutions, J. Colloid Interface Sci., 309 (2007) 126–134.
[34] X. Huangfu, J. Jiang, J. Ma, Y. Liu, J. Yang, Aggregation kinetics of manganese dioxide colloids in aqueous solution: influence of humic substances and biomacromolecules, Environ. Sci. Technol., 47 (2013) 10285–10292.
[35] M. Hudlikar, S. Joglekar, M. Dhaygude, K. Kodam, Green synthesis of TiO_2 nanoparticles by using aqueous extract of *Jatropha curcas* L. latex, Mater. Lett., 75 (2012) 196–199.

[36] G.V. Khade, M.B. Suwarnkar, N.L. Gavade, K.M. Garadkar, Green synthesis of TiO_2 and its photocatalytic activity, J. Mater. Sci. - Mater. Electron., 26 (2015) 3309–3315.
[37] X. Li, M. Yoneda, Y. Shimada, Y. Matsui, Effect of surfactants on the aggregation and stability of TiO_2 nanomaterial in environmental aqueous matrices, Sci. Total Environ., 574 (2017) 176–182.
[38] X. Liu, M. Wazne, Y. Han, C. Christodoulatos, K.L. Jasinkiewicz, Effects of natural organic matter on aggregation kinetics of boron nanoparticles in monovalent and divalent electrolytes, J. Colloid Interface Sci., 348 (2010) 101–107.
[39] Y. Xiang, Y. Liu, B. Mi, Y. Leng, Molecular dynamics simulations of polyamide membrane, calcium alginate gel, and their interactions in aqueous solution, Langmuir, 30 (2014) 9098–9106.